AD-A193 479 BEAM ASSISTED FABRICATION OF III-V/SI MONOLITHIC 1/1
DEVICES(U) COLORADO STATE UNIV FORT COLLINS
G V ROBINSON 31 MAR 88 AFOSR-TR-88-0577
UNCLASSIFIED F49620-86-K-0021 F/G 20/12 NL

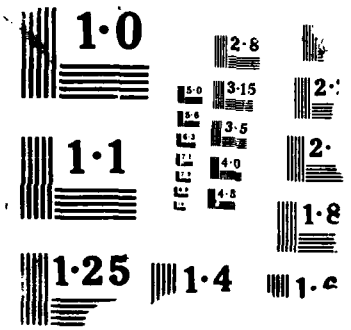
1·0
1·1
1·25
1·4
2·8
3·15
3·5
4·0
4·8
2·
1·8

(2)

AD-A195 479

DTIC ELECTE JUN 29 1988 S D

DTIC FILE COPY

REPORT DOCUMENTATION PAGE

1a. REPORT SECURITY CLASSIFICATION AUTHORITY	1b. RESTRICTIVE MARKINGS
2a. SECURITY CLASSIFICATION AUTHORITY	3. DISTRIBUTION/AVAILABILITY OF REPORT Approved for public release; distribution unlimited.
2b. DECLASSIFICATION/DOWNGRADING SCHEDULE	
4. PERFORMING ORGANIZATION REPORT NUMBER(S)	5. MONITORING ORGANIZATION REPORT NUMBER(S) AFOSR-TR- 88-0577
6a. NAME OF PERFORMING ORGANIZATION: Colorado State University; 6b. OFFICE SYMBOL (If applicable)	7a. NAME OF MONITORING ORGANIZATION: AFOSR/NE
6c. ADDRESS (City, State and ZIP Code): Fort Collins, CO 80523	7b. ADDRESS (City, State and ZIP Code): Bldg 410 Bolling AFB, DC 20332-6448
8a. NAME OF FUNDING/SPONSORING ORGANIZATION: AFOSR/NE; 8b. OFFICE SYMBOL (If applicable)	9. PROCUREMENT INSTRUMENT IDENTIFICATION NUMBER: F49620-86-K-0021
8c. ADDRESS (City, State and ZIP Code): Bldg 410 Bolling AFB, DC 20332-6448	10. SOURCE OF FUNDING NOS.

PROGRAM ELEMENT NO.	PROJECT NO.	TASK NO.	WORK UNIT NO.
61102F	DARPA 5548	00	

11. TITLE (Include Security Classification): Beam Assisted Fabrication of III-V/Si Monolithic Devices

12. PERSONAL AUTHOR(S): Dr. Robinson

13a. TYPE OF REPORT	13b. TIME COVERED	14. DATE OF REPORT (Yr., Mo., Day)	15. PAGE COUNT
Semi-Annual	FROM 01/10/87 TO 31/03/88		

16. SUPPLEMENTARY NOTATION

17. COSATI CODES			18. SUBJECT TERMS (Continue on reverse if necessary and identify by block number)
FIELD	GROUP	SUB. GR.	

19. ABSTRACT (Continue on reverse if necessary and identify by block number)

This research project is to explore two new methods for deposition of III-V semiconducting films on Si substrates. Using gas-source molecular beam epitaxy (MBE) and photo-beam and electron-beam assisted metal-organic chemical vapor deposition (MOCVD), GaAs and other III-V films with abrupt heterojunctions are being formed epitaxially on Si, and by means of optical and electrical Characterization the suitability of the resulting III-V/Si structures are being examined for use in monolithic devices.

20. DISTRIBUTION/AVAILABILITY OF ABSTRACT	21. ABSTRACT SECURITY CLASSIFICATION
UNCLASSIFIED/UNLIMITED ☐ SAME AS RPT. ☐ DTIC USERS ☐	UNCLASSIFIED

22a. NAME OF RESPONSIBLE INDIVIDUAL	22b. TELEPHONE NUMBER (Include Area Code)	22c. OFFICE SYMBOL
MALLOY	(202) 767-4932	NE

DD FORM 1473, 83 APR — EDITION OF 1 JAN 73 IS OBSOLETE.

SECURITY CLASSIFICATION OF THIS PAGE

Semi-Annual Technical Report
(10/1/87 - 3/31/88)

for

AFOSR Contract #F49620-86-K-0021

entitled
"Beam Assisted Fabrication of III-V/Si
Monolithic Devices"

Colorado State University
Fort Collins, CO 80523

P.I. Gary Y. Robinson

Semi Annual Technical Report
(Covering 10/1/87 - 3/31/88)

The objective of this research project is to explore two new methods for deposition of III-V semiconducting films on Si substrates. Using gas-source molecular beam epitaxy (MBE) and photon-beam and electron-beam assisted metal-organic chemical vapor deposition (MOCVD), GaAs and other III-V films with abrupt heterojunctions are being formed epitaxially on Si, and by means of optical and electrical characterization the suitability of the resulting III-V/Si structures are being examined for use in monolithic devices.

Gas-Source MBE (Gary Y. Robinson, Colorado State University)

During this period the testing of the gas-source cracking cell using PH_3 did not take place because of a delay in finishing room remodeling and the longer-than-expected installation of safety warning equipment. However, the gas delivery system was tested using pure H_2 gas and control of gas flow via MBE computer was established. The UHV pumping system was also put into operation.

Meanwhile, to aid in accomplishing our long term objective of fabricating InP/InGaAs heterostructures on Si, we began growing $In_xGa_{1-x}As$ layers lattice matched to InP substrate material. We quickly established control of alloy composition, with x-ray diffraction indicating a mismatch as low as 1.3×10^{-4} (i.e., $x = 0.534 \pm 0.005$) and a low diffraction peak width of 46 arc seconds. Furthermore, Si-doped InGaAs films have exhibited an electron mobility of 8000 $cm^2/V\text{-}s$ at room temperature at an electron concentration of about 1×10^{16} cm^{-3}. Once InP on Si is established, we will use this InGaAs capability for InP/InGaAs on Si.

During this period we began testing of the gas-source MBE system using the gas PH_3. The efficiency of the gas-cracking oven was measured as a function of flow rate and cracking temperature, and the performance of the cracking oven was found to be adequate (about 85-95% efficient) for our initial experiments. The custom-designed gas delivery system worked well with excellent control of gas flow rate. No major problems were encountered with the UHV pumping system, gas scrubber, or safety equipment.

For the first time we deposited InP using gas-source MBE. Both InP substrates and Si substrates were used. The initial results of the InP layer on InP substrates are very encouraging: a single crystal film with a X-ray diffraction peak width at half maximum of 33 arc sec, and a room temperature mobility of 2000 $cm^2/V\text{-}sec$ for Si doping of about $3x10^{17}$ cm^{-3}. These first samples exhibited a high residual impurity (donor) concentration of about $8x10^{16}$ cm^{-3}.

On Si substrates, our first attempt at depositing InP directly without a buffer layer gave mixed results. RHEED patterns faded during InP deposition, indicating lack of crystallinity. Surface morphology varied across the 3-inch diameter wafer from hazy to optically smooth.

More recently, we have succeeded in growing single crystal films of InP on Si using gas-source MBE. The enclosed X-ray rocking curves show two samples: GaAs on Si and InP on Si. The InP films exhibited a n-type residual of about 1 x 10^{17} cm^{-3} and a dislocation density of (4-10) x 10^{9} cm^{-2}.

During the next period, thorough characterization of the InP films will be carried out. Using photoluminescence and SIMS, the residual impurities in the InP layers on InP will be identified. The composition of the InP on Si will be determined with Auger spectroscopy and SIMS and the structure of the film will be determined. Based on the results of the characterization, efforts to grow InP on Si will be continued. If the large lattice mismatch of 8% prevents growth of large area InP single crystal films directly on Si, we will begin exploring the use of buffer layers, such as InGaP, between the InP active layer and the Si substrate.

Energy Assisted MOCVD Deposition (G.J. Collins, Colorado State University).

During this period we ordered the reactor support system and completed the design of the reactor itself. The reactor will be fabricated at the facilities located on site and sent out for welding. Special constraints on the reactor fabrication has been required since substrate temperatures of at least 950°C are required for surface reconstruction. Consideration for heating the substrate without depositing material on the heater have been worked out.

The energy assisted deposition of III-V films focused on the development of a remote hydrogen plasma source in parallel to the efforts to incorporate this technique for the deposition of III-V's on Si. We have demonstrated the plasma source for the deposition of AlN at low temperatures (100°C), as described in the attached publication. We have received the substrate heater system and incorporated it into the design of the GaAs deposition system.

Laser-Assisted MOCVD (Raj Solanki, Subcontract to Oregon Graduate Center).

In the last report, we had briefly described our results of laser induced homoepitaxy of GaP. During the last period, we worked on achieving heteroepitaxy of GaP on Si. The major obstacle here is the removal of the native oxide from silicon in order to achieve epitaxial growth of GaP. We examined two techniques for in situ stripping of the native oxide: thermal desorption and photochemical etching. Of these two, we found the in situ photochemical etching to be simpler and more effective. Following etching, GaP was selectively grown on [100] silicon using the procedure described earlier for homoepitaxy. The GaP microstructures were found to be stoichiometric (Ga - 51%, P - 49%) and single crystal (using TEM). An example of the direct write of GaP on Si is shown below, which is a scanning

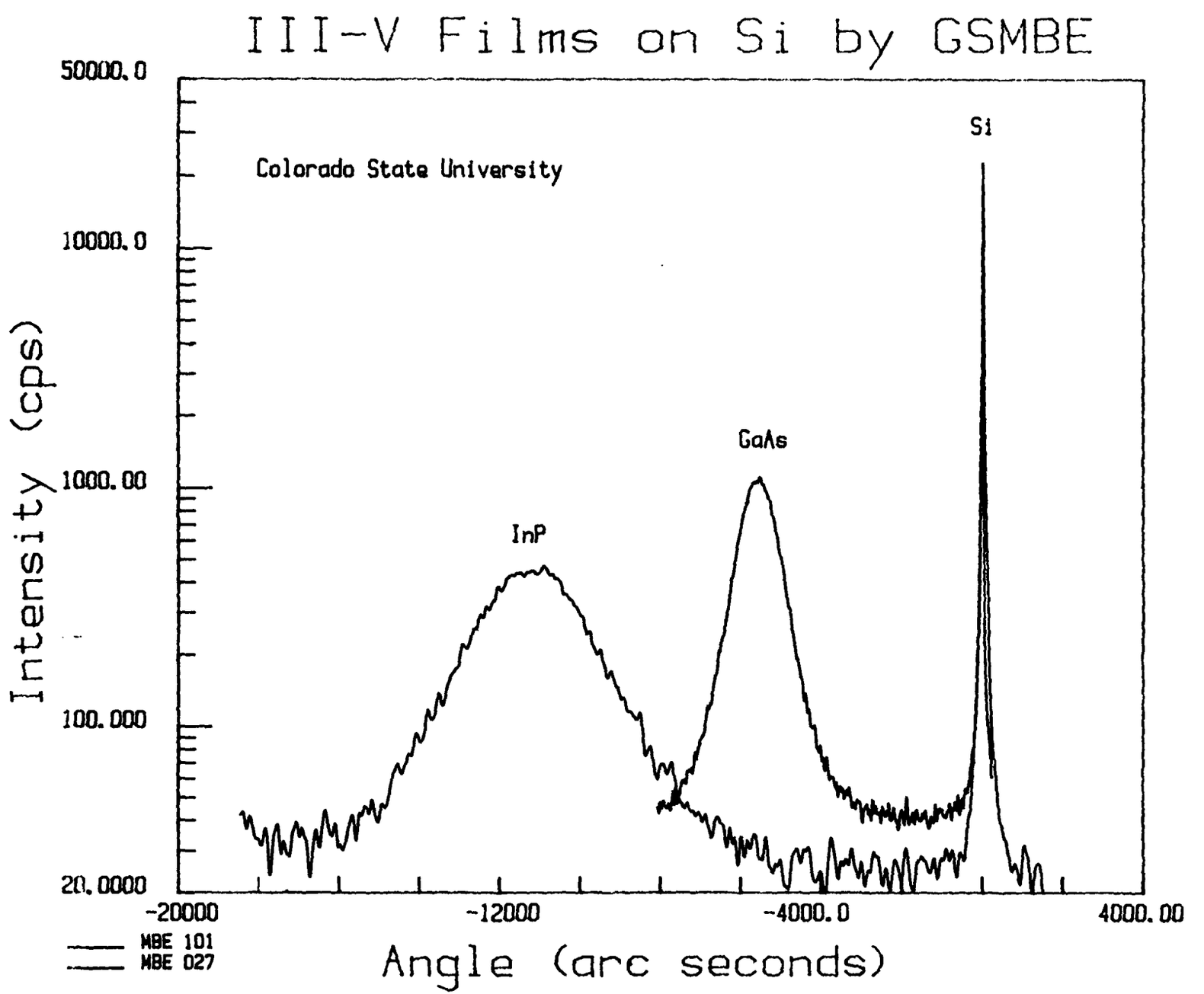
III-V Films on Si by GSMBE
Colorado State University
Si
GaAs
InP
50000.0
10000.0
1000.00
100.000
20.0000
Intensity (cps)
-20000
-12000
-4000.0
4000.00
MBE 101
MBE 027
Angle (arc seconds)

electron micrograph (the marker at the left represents 100 μm). For heteroepitaxy, we have observed that the optimum conditions were different than those for homoepitaxy, especially with respect to the laser power.

To date, we have reported epitaxial growth of GaP on GaP and Si substrates using an argon ion 'direct-write' system. During the last quarter, we continued our investigation to include InP and started deposition of III-V compounds using the UV (excimer) laser system.

InP was selected for laser direct-write since we already had the phosphorous precursor gas (TBP) on the system manifold from our GaP work. For this study, the indium source gas was trimethylindium. The procedure used for direct-write of InP microstructures was the same as that described for GaP. As before, the deposition parameters (III/V ratio, laser power, scan speed) were investigated for homoepitaxy. Stoichiometric films (In 51%, P 49% by Auger analysis) were obtained with III/V ratio as low as 3. Epitaxy was once again checked using transmission electron diffraction mode. Scanning electron micrograph of a patterned InP epitaxial growth is shown in Figure 1a. Its cross-sectional profile measured with a profilometer is shown in Figure 1b. For this deposition, the laser scan speed was 50 μm/s and power of 0.62 W.

Heteroepitaxy of InP on silicon substrates was also investigated. The procedure to remove the native oxide from silicon was described when we reported heteroepitaxy on GaP on Si. After stripping the native oxide, InP lines and pads about 1.8 μm thick were grown on Si. Transmission electron diffraction patterns of these depositions showed the crystalline dot configuration plus rings, indicating presence of a polycrystalline phase. We plan to repeat this investigation at a later date with a GaAs buffer layer on Si in order to distribute the 8% lattice mismatch between InP and Si at the GaAs/Si and GaAs/InP interfaces.

All the III-V depositions we have reported to date have been achieved with an Ar ion laser system. Over this period, we have also been constructing an excimer laser system to obtain III-V epi-growth via photochemical processes. This approach will allow multiple in-situ processes and comparison of the properties of the films grown by the two processes.

One of the obstacles of the photolytic approach is that it requires a means of preventing film growth on the window that lets the UV radiation into the reactor. Over the past few years we have been studying this problem (on a separate project) and have successfully solved it by modifying the gas flow pattern. To date, we have started depositions using this system and are in process of optimizing the process parameters. Moreover, since the photochemical processes involved in the film depositions are unknown, we are also engaged in spectroscopic analysis.

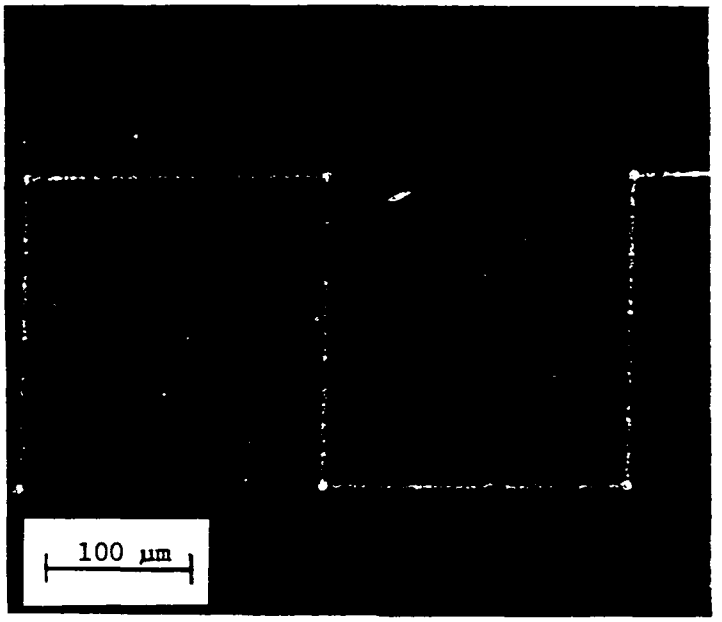

Figure 1a. Laser induced patterned deposition of epitaxial InP on InP subsrates.

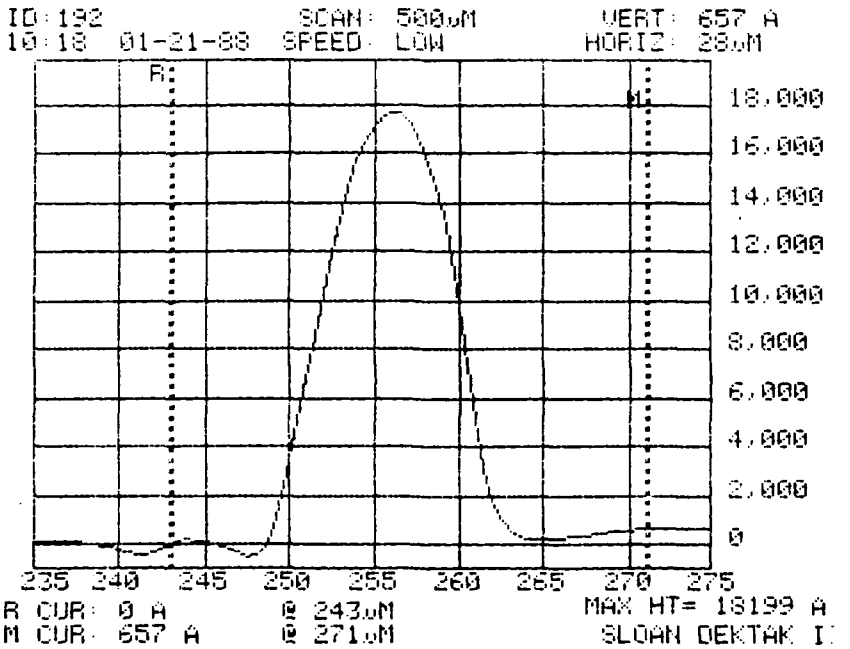

Figure 1b. Cross-sectional profile of the epitaxial growth shown above.

Disk hydrogen plasma assisted chemical vapor deposition of aluminum nitride

T. Y. Sheng, Z. Q. Yu, and G. J. Collins
Department of Electrical Engineering, Colorado State University, Fort Collins, Colorado 80523

(Received 17 September 1987; accepted for publication 16 December 1987)

We employ a well-confined hydrogen plasma of disk shape both as a vacuum ultraviolet (VUV) lamp operating primarily at 121.5 nm and as a source of atomic hydrogen radicals. Both VUV photons and atomic hydrogen act to dissociate feedstock gases used in low-temperature ($<400\,^{\circ}C$) metalorganic chemical vapor deposition (MOCVD). Thin films have been deposited both with the confined hydrogen plasma and with an excimer laser operating at 193 nm in order to compare the two methods. Preliminary chemical and electrical properties of the films deposited via the two methods indicate the superiority of the atomic hydrogen assisted MOCVD technique.

Hydrogen plasmas have been used to dry etch semiconducting materials,[1] deposit GaSb,[2] as well as for hydrogenation and passivation.[3] In a preliminary study, we are exploring the use of a spatially confined hydrogen plasma generated by a disk shaped electron beam as both an *in situ* vacuum ultraviolet (VUV) lamp and as a source of atomic hydrogen.[4] One advantage of the plasma disk is that we may achieve a large area VUV lamp (10–20 cm in diameter) spatially confined in height to less than 1 cm. As a consequence, the plasma is optically thin even for resonance line photons emitted in a direction perpendicular to the disk. This VUV lamp also operates without the need for optical windows; hence, ground state and excited hydrogen atoms created in the plasma disk can diffuse from the plasma disk towards the substrate. It is noteworthy that the ground state $H(1s)$ atomic species that do not heterogeneously recombine into H_2, can be repeatedly optically excited by resonance radiation at 121.5 nm originating from the plasma disk to form excited atomic hydrogen near the substrate surface.

The atomic hydrogen VUV radiation originating from the plasma disk may directly photodissociate polyatomic molecules, which absorb strongly in the VUV region. The unimpeded flow into the reaction chamber of excited and ground state hydrogen species created in the plasma disk creates additional volume dissociation processes for polyatomic feedstock gases. For example, excited $H(2p)$ atoms can participate in sensitized atom-molecule volume reactions such as $H(2p)$ + polyatomic $\rightarrow H(1s)$ + fragments. The ground state hydrogen can also participate in insertion reactions that may dissociate some polyatomic molecules. In short, hydrogen plasma assisted chemical vapor deposition (CVD) provides a new low-temperature fabrication method that opens new dissociation pathways and new means for providing energy to surfaces without charged particle impingement as well as the additional benefits of hydrogenation and passivation.

UV-photo chemical vapor deposition (UV-CVD) is one low-temperature process used successfully in the past to deposit metals, insulators, and semiconducting films.[5–8] In prior UV-CVD the photons were created using mercury lamps operating in the ultraviolet, as well as commercial excimer lasers. The photon energies available, 4–7 eV, from these light sources are in some cases inadequate for directly dissociating some feedstock reactant gases because the photon absorption cross sections of many polyatomic reactant gases used in CVD have peak values in the VUV region beyond the range of both conventional mercury lamps and excimer lasers. The problems for conventional VUV lamps include: the need for a VUV window with high optical transmission, the problem of undesired window deposits, and lack of a wide area (>100 cm^2) illumination source. For excimer laser based CVD, besides the optical window problems, we have: the high laser cost, the daily maintenance requirements, and the small area of the laser beam (2×4 cm) compared to substrate size (10–20 cm in diameter). All of the above limitations act in concert to inhibit use of UV-CVD especially in a manufacturing environment.

Robertson and Milne recently employed an internal discharge lamp[9] using a thermionic electron source for photo-CVD; but it was not possible to achieve large area deposits of acceptable film thickness uniformity. To our knowledge commercial VUV lamps with diameters greater than several cm^2 are simply not available. Hence, there is a well recognized need in photo-CVD technology for an *in situ* VUV lamp that operates without windows, is of large area, and has a uniform intensity profile. The confined hydrogen plasma disk[4] addresses all of these issues.

The schematic diagram of the combined VUV lamp and sensitized reaction assisted metalorganic chemical vapor deposition (MCCVD) apparatus is shown in Fig. 1. A ring shaped cold cathode 8 mm thick and 75 mm in diameter creates an electron beam pumped disk plasma. The plasma disk was located in the present experiments about 10 cm away from the substrate upon which thin films are deposited. The characteristic photon emission spectrum from this hydrogen plasma disk lamp was measured by a VUV monochromator (ARC model VM-502) and was found to be dominated by the atomic hydrogen Lyman-alpha line. The plasma disk structure is windowless as shown in Fig. 1, so that both ground state and excited state atomic hydrogen created in the plasma disk flow unimpeded towards the substrate.

Aluminum nitride (AlN) films have been deposited using hydrogen disk plasma assisted MOCVD. The substrates

 0003-6951/88/070576-03$01.00

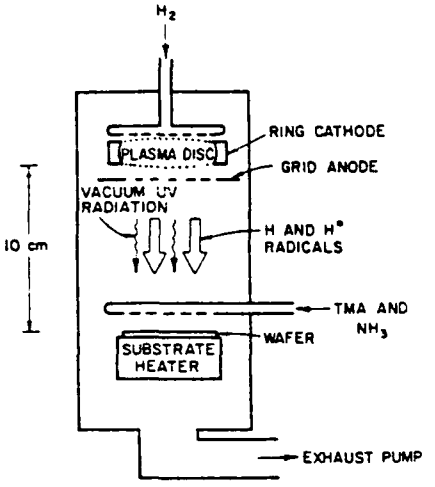

FIG. 1. Schematic diagram of the confined hydrogen plasma disk assisted CVD apparatus. Note that both VUV photons and H radicals emerge from the plasma disk and impinge on the substrate.

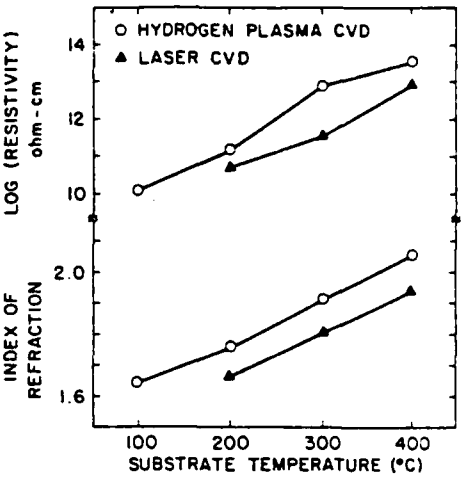

FIG. 2. Electrical resistivity and index of refraction of excimer laser and hydrogen plasma assisted MOCVD of AlN films as a function of substrate temperature.

we used include Si, InP, and GaAs. Feedstock gases of trimethylaluminum (TMA) and ammonia (NH_3) were introduced by a gas manifold located just above the substrate but downstream from the disk shaped hydrogen discharge. Both VUV photodissociation and sensitized hydrogen reactions act to decompose feedstock gases in this arrangement. Details of TMA and NH_3 photodissociation pathways have been studied previously[10] but little is known about excited state hydrogen sensitized reactions with TMA and NH_3.

Experimental conditions for the hydrogen disk plasma assisted AlN film deposition are summarized in Table I. The deposition rate varied from about 20 nm/min for 400 °C substrate temperature to about 5 nm/min for 100 °C substrate temperature. It is noteworthy that deposited film thickness variation is within 5% over the entire disk plasma area.

The AlN electrical properties measured include film resistivity and dielectric constant. The refractive index of deposited AlN films was also measured by a conventional ellipsometer operating at 633 nm. Figure 2 compares both the electrical resistivity and refractive index of AlN films deposited employing either the hydrogen disk plasma or an ArF* excimer laser beam.[11] At the same deposition temperature, AlN films deposited by the hydrogen plasma assisted CVD show higher electrical resistivity and higher refractive index. Note that with hydrogen plasma CVD we can deposit good quality AlN films at 100 °C whereas the laser-CVD technique is not able to do so. AlN deposited at 400 °C with hydrogen disk plasma VUV lamp CVD exhibit a resistivity similar to that reported for bulk AlN ($>5\times10^{13}$ Ω cm).[12]

Chemical properties of the film were examined by Auger electron spectroscopy (AES) and infrared absorption spectroscopy (FTIR) to examine the elemental Al/N ratio and N–H bonding in the film, respectively. Both disk hydrogen plasma and laser-CVD films have nearly equivalent aluminum to nitrogen ratios, being approximately 1. Compared to conventional thermal MOCVD AlN films, hydrogen disk plasma CVD AlN films possess twice the carbon contamination as determined by secondary ion mass spectroscopy analysis. Oxygen content in the hydrogen plasma assisted CVD AlN films varied from 5% when employing a 100 °C substrate temperature to less than 1% for a 400 °C substrate temperature as determined by AES. With the same substrate temperature (above 200 °C), the oxygen content is 2% higher in laser deposited films than in the hydrogen disk plasma deposited films. FTIR absorbance spectra of disk plasma assisted CVD AlN samples were examined in the spectral range 4400–400 cm^{-1}. The spectrum shows three well-known peaks around 610, 655, and 670 cm^{-1}, as discussed in Ref. 13. These three peaks exhibit increased intensity and sharpen in shape with increasing substrate temperature. The absorption band around 460 cm^{-1} was observed for films deposited at low temperature but nearly disappeared when the deposition temperature is higher than 350 °C. This behavior is consistent with the identification of the absorption peak at 460 cm^{-1} as a vibrational mode of the Al_2O_3 molecule.[14] These results also support the AES analysis of residual oxygen in AlN films. The absorption peak centered around 3340 cm^{-1} is associated with the N–H stretching mode. The integrated peak area is the same for all hydrogen plasma deposited samples regardless of varying substrate temperature. Whereas, in the laser CVD films, the area of the N–H band is much larger for samples deposited at low temperature (200 °C) but decreases dramatically with increasing substrate temperatures as shown in Fig. 3. The wet etch rate at 60 °C of photo-CVD AlN in 85% phosphoric acid (H_3PO_4) is also shown in Fig. 3. Plasma disk deposited

TABLE I. Disk hydrogen plasma assisted deposition conditions for AlN films.

Light source	H_2 discharge (10.2 eV)
Ring cathode potential	− 500 V
Grid anode potential	20 V
H_2/NH_3/TMA flow ratio	200/60/1.5
Substrate temperature	100–400 °C
Total reactor pressure	1 Torr

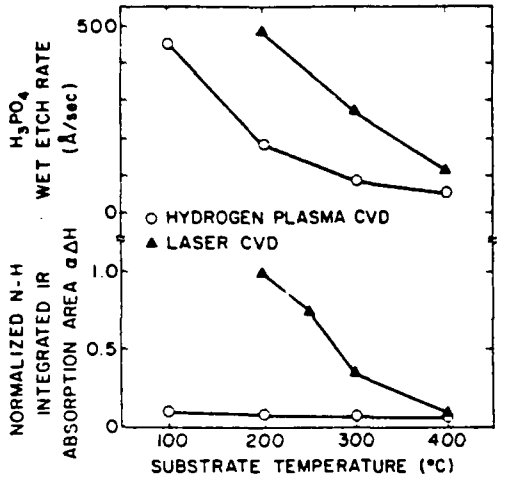

FIG. 3. Variation of N–H bonding of deposited AlN films and the wet etch rate at 60 °C in 85% H_3PO_4 as a function of substrate temperature for both hydrogen plasma and excimer laser assisted MOCVD.

AlN films show a 2–3 times lower etch rate, indicating both the lower hydrogen content and the higher film density.

In conclusion, hydrogen disk plasma assisted CVD results in higher quality AlN films at lower substrate temperature than laser CVD. It is judged that impinging H and H* atoms on the AlN film help maintain AlN film properties at lower substrate temperature[15] by providing additional energy to the surface. The lower refractive index and lower resistivity observed for photoassisted CVD films as compared to bulk AlN is judged due to both the lower film density and the small amount of oxygen and hydrogen incorporated in the films. It is also practically noteworthy that the hydrogen plasma disk assisted CVD technique can deposit uniform thickness films over large area with VUV lamp power constant over hundreds of hours.

This research was supported in part by the Defense Advanced Research Projects Agency, Applied Electron, and the Naval Research Laboratory.

[1]R. P. H. Chang, C. C. Chang, and S. Darack, J. Vac. Sci. Technol. **20**, 45 (1982).
[2]Y. Sato, K. Matsushita, T. Hariu, and Y. Shibata, Appl. Phys. Lett. **44**, 592 (1984).
[3]W. C. Dautremont-Smith, J. C. Nabity, V. Swaminathan, M. Stavola, J. Chevallier, C. W. Tu, and S. J. Pearton, Appl. Phys. Lett. **49**, 1098 (1986). See also S. J. Pearton, C. S. Wu, M. Stavola, J. Lopata, W. C. Dautremont-Smith, S. M. Vernon, and V. Haven, Appl. Phys. Lett. **51**, 496 (1987).
[4]VUV lamp source provided by Applied Electron Corp., Albuquerque, NM; U. S. Patent No. 4 509 451 (1985) and others pending.
[5]D. J. Ehrlich, R. M. Osgood, Jr., and T. F. Deutsch, J. Vac. Sci. Technol. **21**, 83 (1982).
[6]V. M. Donnelly, D. Brasen, A. Appelbaum, and M. Geva, J. Appl. Phys. **58**, 2022 (1985).
[7]H. Ando, H. Inuzuka, M. Konagai, and K. Takahashi, J. Appl. Phys. **58**, 802 (1985).
[8]A. Yamada, M. Konagai, and K. Takahashi, Jpn. J. Appl. Phys. **24**, 1586 (1985).
[9]P. A. Robertson and W. I Milne, *Proceedings of the Fall MRS Conference in Boston* (Materials Research Society, Pittsburgh, 1986), p. 88.
[10]D. J. Ehrlich, R. M. Osgood, Jr., and T. F. Duetsch, IEEE J. Quantum Electron. **QE-16**, 1233 (1980). See A. W. Laubengayer, J. D. Smith, and G. G. Ehrlich, Am. Chem. Soc. **83**, 542 (1961). See V. M. Donnelly, A. P. Barowavski, and J. R. McDonald, Chem. Phys. **213**, 218 (1979). See also D. Eres, T. Motooka, S. Gorbatkin, D. Lubben, and J. E. Greene, J. Vac. Sci. Technol. B **5**, 848 (1987).
[11]C. A. Moore, Z. Q. Yu, L. R. Thompson, and G. J. Collins, in *Handbook of Thin Films Deposition Processes and Technologies*, edited by K. Schuegraf (Noyes, Parkridge, NJ, 1987), Chap. 10.
[12]Y. Kurokawa, K. Utsumi, H. Takamizawa, T. Kamata, and S. Noguchi, IEEE Trans. Components, Hybrids, Manuf. Technol. **CHMT-8**, 247 (1985).
[13]A. T. Collins, E. L. Lightowlers, and P. J. Dean, Phys. Rev. **833**, 158 (1967).
[14]A. Takase, S. Umebayashi, and K. Kishi, Jpn. J. Appl. Phys. **21**, 1447 (1982).
[15]W. R. Knolle, H. R. Maxwell, and R. E. Beneson, J. Appl. Phys. **51**, 4385 (1980).

END
DATED
FILM
8-88
DTIC